2004

Comparison of long term cochlear noise injury and age-related cochlear degeneration in mice

Ashlea Joann Wyrick

COMPARISON OF LONG TERM COCHLEAR NOISE INJURY AND AGE-RELATED COCHLEAR DEGENERATION IN MICE

By

Ashlea Joann Wyrick

An independent study submitted in partial
fulfillment of the requirements for the degree of:

Master of Science in Speech and Hearing

Emphasis in Audiology

Washington University
Department of Speech and Hearing

May 21, 2004

Approved by:
Kevin Ohlemiller, Ph.D, Independent Study Supervisor

Comparison of Long Term Cochlear Noise Injury and Age-related Cochlear Degeneration in Mice

Introduction

The interaction of age-related hearing loss (ARHL) and noise-induced hearing loss (NIHL) is complex and not readily understood Rosenhall (2003). ARHL appears in over 40% of the population over the age of 65 National Center for Health Statistics (1994). It is poorly understood because it is difficult to separate the genetic and environmental contributors. Schuknecht (1964, 1993) and Schuknecht and Gacek (1993) proposed categories for ARHL in humans. *Sensory* ARHL, one of Schuknecht's categories, shows many of the same features as NIHL. Both *sensory* ARHL and NIHL principally comprise degeneration of the organ of Corti.

The purpose of this study is to look at different cell types that are affected by aging and noise and determine if those changes are similar. While this issue has been addressed before, we sought to take advantage of newly recognized cellular changes. These include changes in fibrocytes of the limbus and lateral wall, as well as subtle changes within the organ of Corti Hequembourg and Liberman (2001, Ohlemillear and Gagnon (2004) and Wang et al. (2002). The present study addresses the following questions: (1) Is noise injury, as determined by ABR threshold shifts, stable over long periods of time?, (2) Is noise injury, as determined by histopathology, stable?, (3) When noise exposed animals are allowed to age and compared with non-exposed age-matched controls, are the ABR threshold shifts and histological changes independent, or alternatively, does one form of pathology exacerbate or inhibit the other?, and (4) When noise-exposed animals are compared to aging animals, how similar is the pathology? We compared ABR thresholds and quantitative histopathology in noise exposed CBA/CaJ mice and age-matched unexposed controls for one year post exposure. Histopathological analysis

included measures of spiral ganglion cells, spiral limbus fibrocytes, fibrocytes within the spiral ligament (Type II and IV), and the presence or absence of supporting cell pathology as described by Ohlemiller and Gagnon (2004). Thickness measures were also obtained for the stria vascularis and the spiral ligament.

Materials and Methods

Animals

The study included 34 male CBA/CaJ mice. The animals were divided into noise exposed and non-noise exposed groups. The noise exposed group consisted of three groups, all the groups were noise exposed at six months. Six mice were sacrificed one month post-noise exposure, nine mice were sacrificed at six months post-noise exposure, and seven animals were sacrificed at 12 months post-noise exposure. Non-noise exposed controls included five mice that were sacrificed at four months and seven mice that were sacrificed at 18 months. All mice underwent ABR recording of the right ear prior to exposure, one month post-exposure, and at six month intervals thereafter.

Noise Exposure

Noise exposure and auditory brainstem response (ABR) recordings were performed in a foam-lined, single-walled soundproof room (Industrial Acoustics, Bronx, NY) Ohlemiller et al. (2000). Mice were exposed in pairs to 110 dB SPL of broadband noise for two hours. Noise was generated by General Radio 1310 generators and bandpassed at 4.0-45.0 kHz by Krohn-Hite 3550 filters.

ABR Recordings

Auditory brainstem response (ABR) thresholds were obtained at 5, 10, 20 28.3, and 40 kHz as described in detail elsewhere Ohlemiller et al. (2002).

Histology

Each mouse was sacrificed within one week after their last ABR recording. Mice were overdosed and perfused transcardially with cold 2.0% paraformaldehyde/ 2.0% glutaraldehyde in 0.1 M phosphate buffer (pH 7.4). Each cochlea was isolated rapidly and immersed in the same fixative, and the stapes was removed immediately. The cochleas were infiltrated completely by fixative by making a small hole in the cochlear capsule and circulating the fixative (using a transfer pipette) over the cochleas. After the cochlea's decalcified in sodium EDTA for 72 hours, they were postfixed in buffered 1% osmium tetroxide, dehydrated in an ascending acetone series, and embedded in Araldite Ohlemiller and Gagnon (2004). Each cochlea was then sectioned at 4 μm thick in the midmodiolar plane and stained with toluidine blue.

Morphometry

Measures were obtained for spiral ganglion cells, limbus fibrocytes, fibrocytes within the spiral ligament (Type II and IV), and presence or absence of abnormal supporting cell profiles. In addition, thickness was measured for the stria vascularis and spiral ligament. Each measurement was obtained at 400x by light microscope examination with a calibrated ocular. Every fourth section was examined. Measures were obtained in the lower apex (corresponding roughly to the 5 kHz region), upper base (10 kHz region), and lower base (40 kHz region) of the cochlea.

Neuronal counts

Spiral ganglion cell counts were obtained using a 3,600 μm^2 area centered in Rosenthal's canal. Only nucleated profiles lying mostly within the grid were counted.

Fibrocytes counts

A 1,600 μm^2 grid was used to count primarily stellate fibrocytes in the limbus, Type II, and Type IV fibrocyte in the spiral ligament. Counts were obtained by centering the grid in the regions depicted in Figure 1A. Type II fibrocytes counts were obtained by placing the grid just behind the spiral prominence. Type IV fibrocyte counts were obtained by placing the 1,600 $\square m^2$ grid directly lateral to the Basilar membrane. Fibrocytes were classified by their location as previously described Ohlemiller and Gagnon (2004).

Stria vascularis and ligament thickness

Stria vascularis thickness was measured at the midpoint, perpendicular to the long axis of the epithelium. Ligament thickness was measured immediately adjacent to the stria's midpoint on the same axis. Figure 1A illustrates a typical measurement axis.

Supporting cell analyses

For each location the condition of supporting cells in the organ of Corti was determined by the appearance of abnormal supporting cells (Claudius, Hensen, and tectal cells). Abnormality of the supporting cells was defined as the having distinctive staining patterns and unusual shapes Ohlemiller and Gagnon (2004). Figure 1A exemplifies the appearance of dark supporting cells.

Data analysis

Foe each animal the measures that were obtained were averaged so that for each animal there was a single average for each cell type. For each cell type and location the data obtained were analyzed by one-way ANOVA with Holm-Sidak multiple comparison testing. Overall differences were considered significant if the one-way ANOVA results were significant at a level of $p < 0.001$. The differences between groups were considered significant if the Holm-Sidak comparisons showed differences between groups at the level of $p < 0.05$.

Results

ABR thresholds

Mean ABR threshold shifts at various times post-exposures for each frequency are shown in Figure 2. Post-noise exposure, the mice show a shift in thresholds at all frequencies, with the most notable shifts occurring at 20 kHz, 28.3 kHz, and 40 kHz. All additional shifts accruing with time post-exposure appear to be due to aging, as evident by the parallel trajectory of changes over time in exposed and non-exposed animals. This indicates that there is an additive effect of noise exposure and age.

Neuronal counts

Figure 3 shows spiral ganglion cell loss by experimental group in each region. Significant differences were found between the control groups and within the post-exposure groups. No difference was observed in non-noise exposed young controls and the one month noise exposed groups. The data suggest there is primarily an aging affect in all locations of the cochlea. In the lower apex, aging appears to be independent. In the upper and lower base both aging and noise were associated with neuronal loss but the data are ambiguous with regard to any interaction between these.

Fibrocytes counts

Figure 4 shows that, within the limbus fibrocytes, age and noise both seem to affect the cells in the lower apex and the lower base. In the upper base there appears to be an aging affect. However, there does not seen to be an additive effect of either the noise or aging on the limbus fibrocytes. In the lower apex and upper base there is a significant difference between the four month control group and the 18 month controls, as well as the post-exposure groups. Within the Type II fibrocytes there appears to be primarily an aging effect within all three cochlear regions (Figure 5). There is a significant difference between the 18 month controls and the one month post-exposure (all regions), six month post-exposure (lower and upper base), and the one year controls (all regions). In the upper and lower base there is a significant difference between both control groups and all three post-exposure groups. There appears to be an independent and additive affect of noise and aging in the Type IV fibrocytes (Figure 6). As one example, using the young control as a reference, the loss of fibrocytes in the 18 month controls added to the loss

of the one month post-exposure approxiamately equals the loss obtained by the one year post-exposure group.

Stria vascularis and ligament thickness

There did not seem to be any tendency of noise or aging to reduce the thickness of either the stria vascularis or ligament thickness. Within the stria vascularis there is some evidence that noise injury progresses with time in all three locations (Figure 7). There appears to be a counter effect of both noise and age in the ligament thickness across all regions (Figure 8).

Supporting cell analyses

The type of supporting cell anomalies reported by Ohlemiller and Gagnon (2004) were observed in all cochlear locations. As shown by Figure 9, the odds of observing these greatly increased with noise exposure, but appeared unchanged by aging.

Discussion

NIHL has been studied in great detail. Many of the studies looked at the results around one to two week post-noise exposure and inferred that the hearing loss was stable. This study examined the hearing of the CBA/CaJ mouse one month, six month, and one year post-noise exposure.

Stability of noise injury: ABR thresholds

ABR thresholds obtained pre and post-noise exposure indicated that the noise injury to the mice were stable. The changes in the thresholds post-noise appeared primarily due to aging.

For each of the frequencies presented, the shift in thresholds that occurred were parallel to changes over time; thus indicating that a fixed noise injury contribution was added to a cumulative aging effect.

Stability of noise injury: Histopathology

Within the spiral ganglion cell and Type II fibrocytes the noise injury appeared stable. There did not appear to be any difference in neuronal loss between the six month and the one year post-noise exposed mice in all cochlear regions. If the noise injury was not stable then we would expect to see a greater loss due to aging than what was found. The six month post-noise exposed mice and the one year controls within the Type II fibrocytes appear to be similar in the amount of cell loss across all regions measured.

Relation between ARHL and NIHL

When the ABR thresholds are compared we observed an aging effect. This can be seen in the fact that the changes in thresholds over time were parallel in very frequency tested in each of the noise exposed mice.

We observed that noise and aging minimally affected the stria vascularis. Wang et al. (2002) reported noise exposure did affect the stria vascularis. They noted that the stria became swollen after an exposure of 116 dB noise band. Hequembourg and Liberman (2001) suggested significant changes in the spiral ligament and the stria vascularis in regard to age with C57BL/6 mice. Also, we observed a minimal affect of noise and aging on the spiral ligament. It is possible that when the mice age that aging causes the ligament to become thicker.

The changes that occurred within the Type IV fibrocytes appear to be an additive effect of noise and age. In the upper and lower base we observed that the cell loss in the one month noise exposed mice and the 18 month control mice equal the amount of cell loss for the 18 month old noise exposed mice. Hequembourg and Liberman (2001) noted that with increasing age the first noticeable cell loss was the Type IV fibrocytes and much less severe in the Type II. Wang et al. (2002) reported degeneration in the Type IV fibrocytes with noise exposure.

The changes that we observed in the Type II fibrocytes appear to be primarily aging. Hequembourg and Liberman (2001) also found that with aging Type II fibrocytes were damaged as well.

We found that the dark supporting cells were affected primarily by noise across all regions of the cochlea.

Are noise and aging equivalent?

We observed that noise and aging appears to be equivalent in every measure and thicknesses obtained expect the Type IV fibrocytes. Within the Type IV fibrocytes there was no significant affect of aging alone.

Conclusion

Noise injury appears to be stable in all cell types examined. Aging and noise are largely independent of one another. ARHL and NIHL appear to be the same except for the Type IV fibrocytes, stria vascularis thickness, and supporting cell anomalies; however overall literature supports the similarity of all three.

Legends

Figure 1A: Illustrates locations of cell types and thickness obtained; 1B illustrates missing limbus fibrocytes and missing spiral ganglion neurons

Figure 2: ABR threshold changes overtime for frequencies tested for noise exposed group's pre and post-noise exposure

Figure 3: Cell density obtained for group and age (* indicates $p < 0.05$ using the young controls as a reference)

Figure 4: Cell density obtained within Rosenthal's canal (* indicates $p < 0.05$ using the young controls as a reference)

Figure 5: Cell density obtained for group and age (* indicates $p < 0.05$ using the young controls as a reference)

Figure 6: Cell density obtained for group and age (* indicates $p < 0.05$ using the young controls as a reference)

Figure 7: Thickness obtained for group and age (* indicates $p < 0.05$ using the young controls as a reference)

Figure 8: Thickness obtained for group and age (* indicates $p < 0.05$ using the young controls as a reference)

Figure 9: Supporting cell anomalies (* indicates $p < 0.05$ using the young controls as a reference)

References

Hequembourg S, Liberman MC. 2001. Spiral ligament pathology: a major aspect of age-related cochlear degeneration in C57BL/6 mice. *J Assoc Res Otolaryngol* 2:118-129.

National Center for Health Statistics. 1994. Prevalences and characteristics of persons with hearing trouble. Washington, DC: Department of Health Human Serviecs, Public Health Service.

Ohlemiller KK, Gagnon PM. 2004. Cellular correlates of progressive hearing loss in 129S6/SvEv mice. *J Comp Neurol* 469:377-390.

Ohlemiller KK, McFadden SL, Ding D-L, Lear PM, Ho Y-S. 2000. Targeted mutatin of the gene for cellular glutathione peroxidase (G*px*1) increases noise-induced hearing loss in mice. *J Assoc Res Otolaryngol* 1:243-254.

Rosenhall U. 20023. The influence of aging on noise-induced hearing loss. *Noise & Health* 20:47-53.

Schuknecht HF. 1964. Further observations on the pathology of presbycusis. *Arch Otolaryngol* 80:369-382.

Schuknecht HF. 1993. Pathology of the ear. Philadelphia : Lea & Febiger.

Schuknecht HF, Gacek MR. 1993. Cochlear pathology in presbycusis. *Ann Otol Rhinol Laryngol* 102:1-16.

Wang Y, Hirose K, Liberman MC. 2002. Dynamics of noise-induced cellular injury and repair in the mouse cochlea. *J Assoc Res Otolaryngol* 3:248-268.

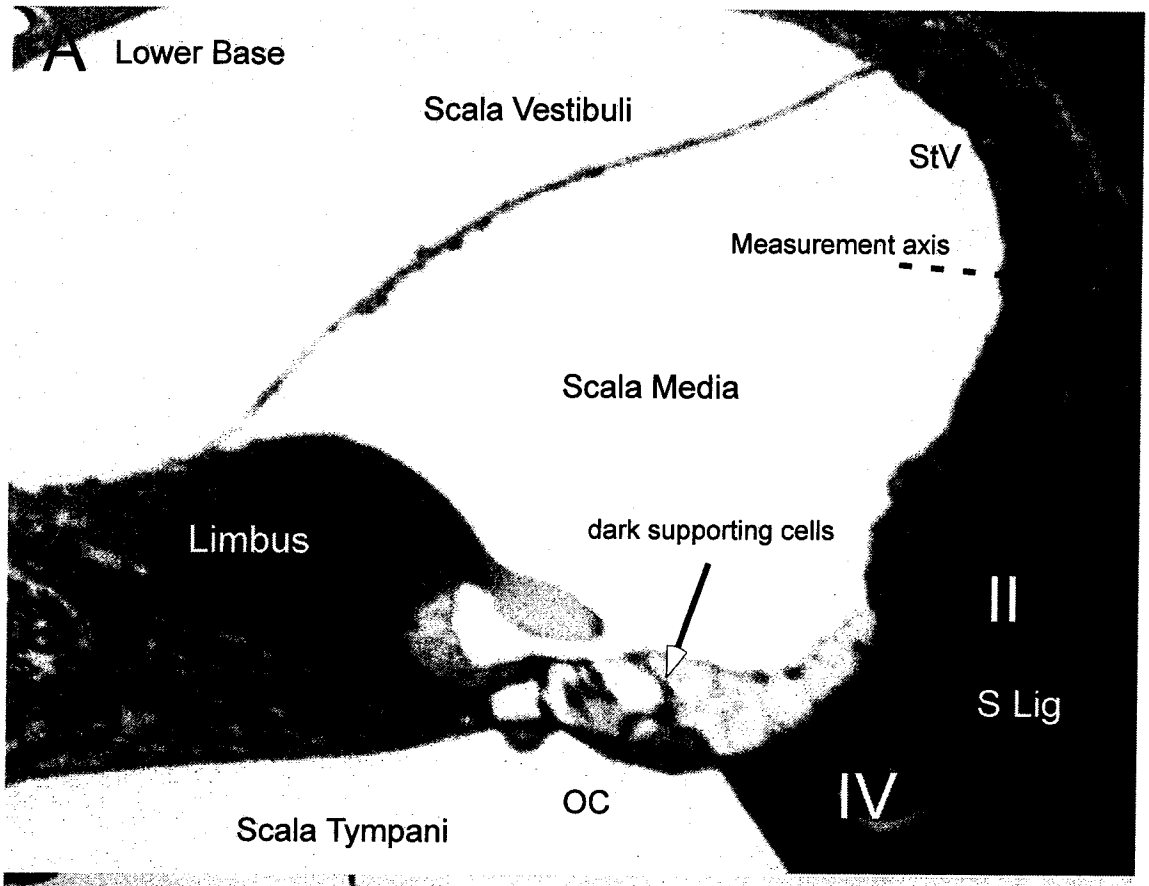
A Lower Base
Scala Vestibuli
StV
Measurement axis
Scala Media
Limbus
dark supporting cells
II
S Lig
IV
OC
Scala Tympani

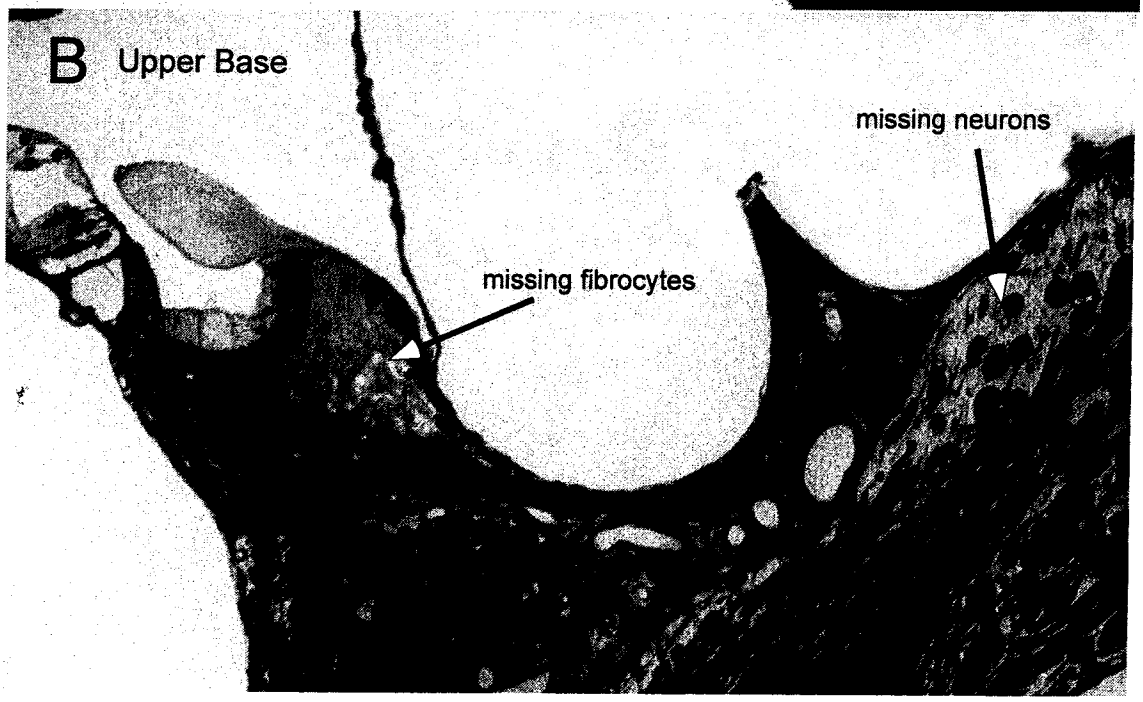
B Upper Base
missing neurons
missing fibrocytes

Figure 2

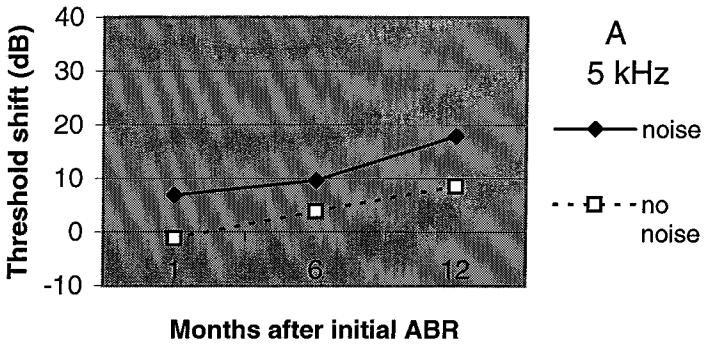

A

5 kHz

noise

no noise

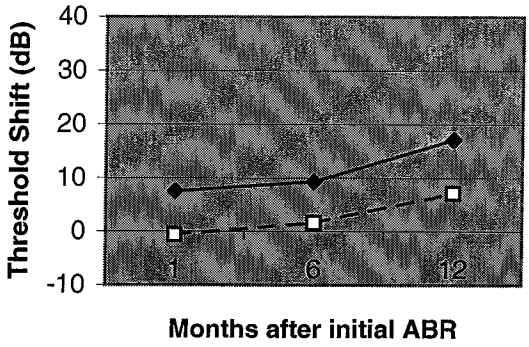

B

10kHz

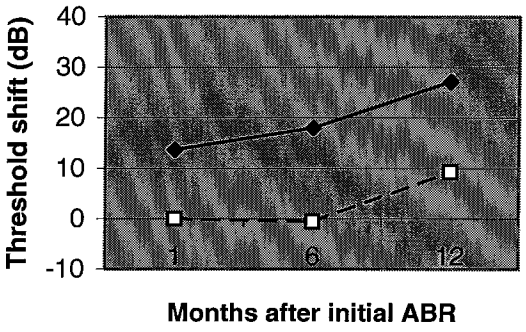

C

20 kHz

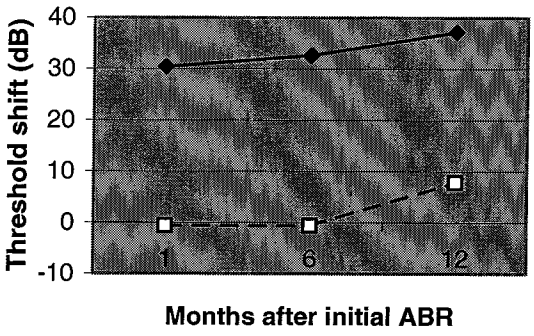

D

28.3 KHz

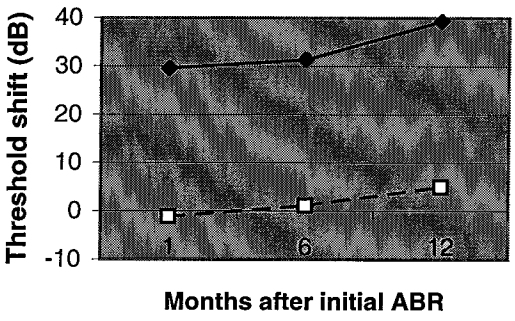

E

40 kHz

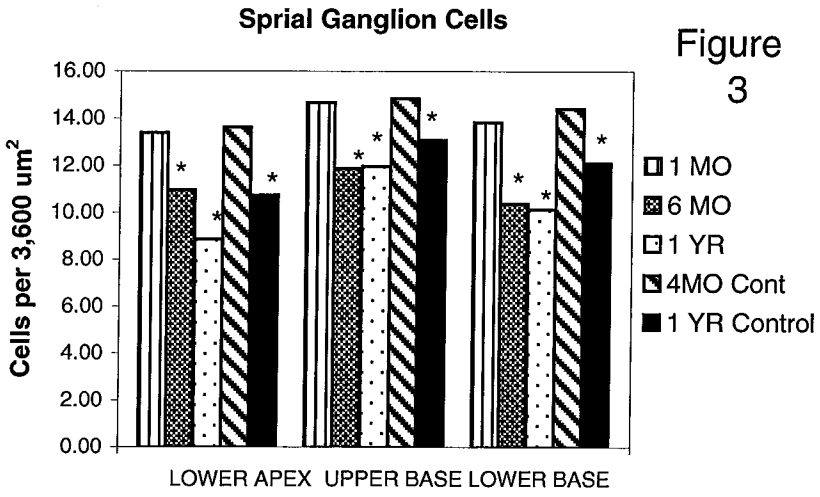
Sprial Ganglion Cells
Cells per 3,600 um2
16.00
14.00
12.00
10.00
8.00
6.00
4.00
2.00
0.00
LOWER APEX
UPPER BASE
LOWER BASE
1 MO
6 MO
1 YR
4MO Cont
1 YR Control

Figure 3

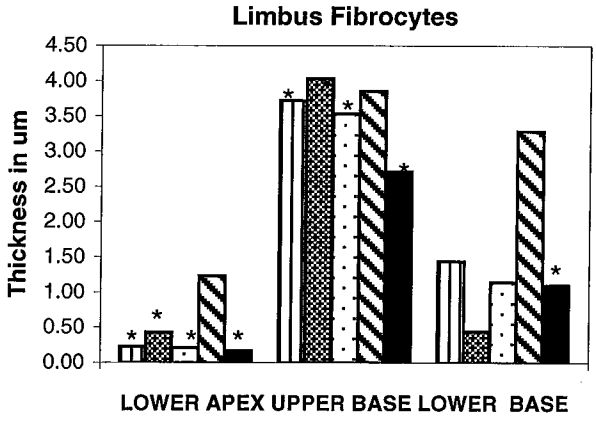
Limbus Fibrocytes
Thickness in um
4.50
4.00
3.50
3.00
2.50
2.00
1.50
1.00
0.50
0.00
LOWER APEX
UPPER BASE
LOWER BASE

4

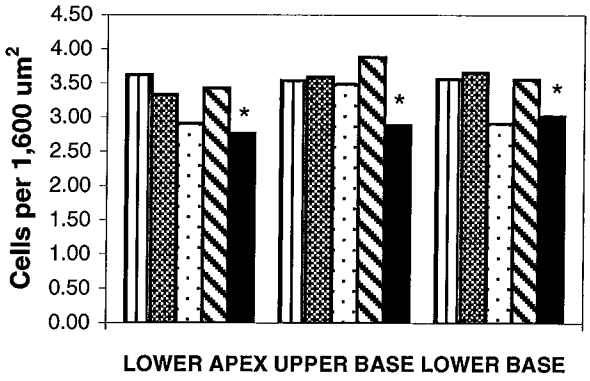
Type II Fibrocytes
Cells per 1,600 um2
4.50
4.00
3.50
3.00
2.50
2.00
1.50
1.00
0.50
0.00
LOWER APEX
UPPER BASE
LOWER BASE

5

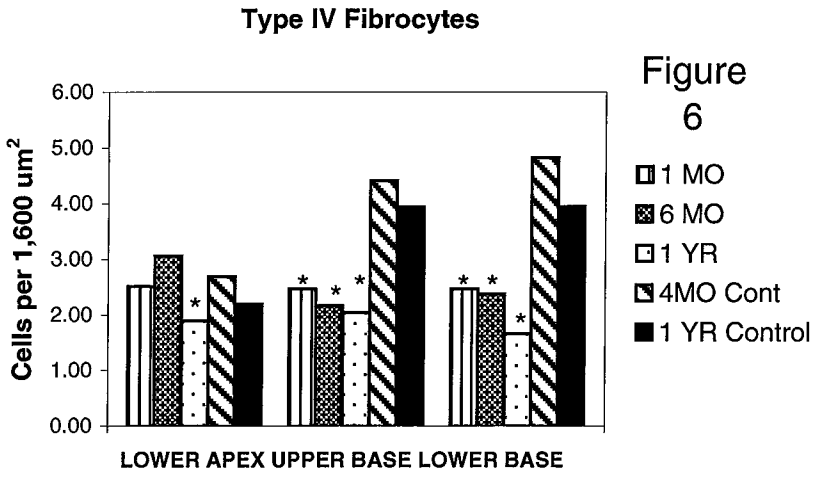
Type IV Fibrocytes
Cells per 1,600 um2
6.00
5.00
4.00
3.00
2.00
1.00
0.00
LOWER APEX UPPER BASE LOWER BASE
1 MO
6 MO
1 YR
4MO Cont
1 YR Control

Figure 6

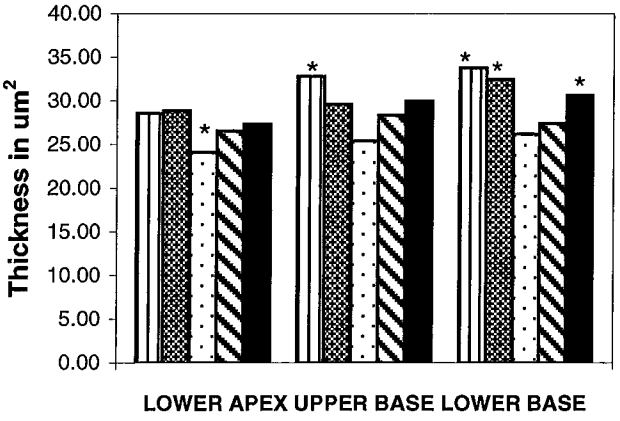
Stria vascularis
Thickness in um2
40.00
35.00
30.00
25.00
20.00
15.00
10.00
5.00
0.00
LOWER APEX UPPER BASE LOWER BASE

7

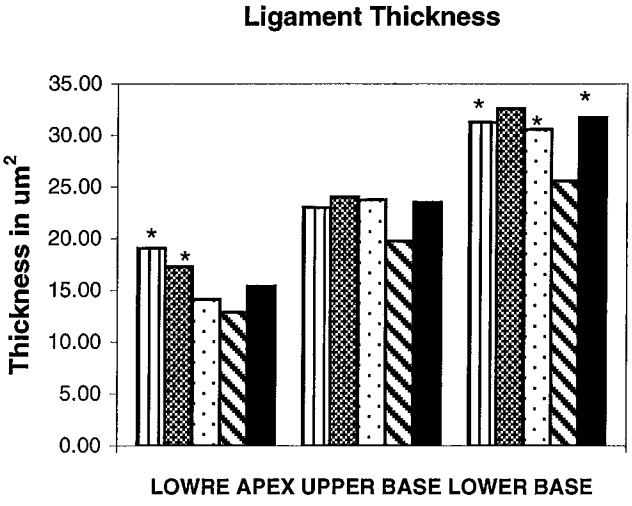
Ligament Thickness
Thickness in um2
35.00
30.00
25.00
20.00
15.00
10.00
5.00
0.00
LOWRE APEX UPPER BASE LOWER BASE

8

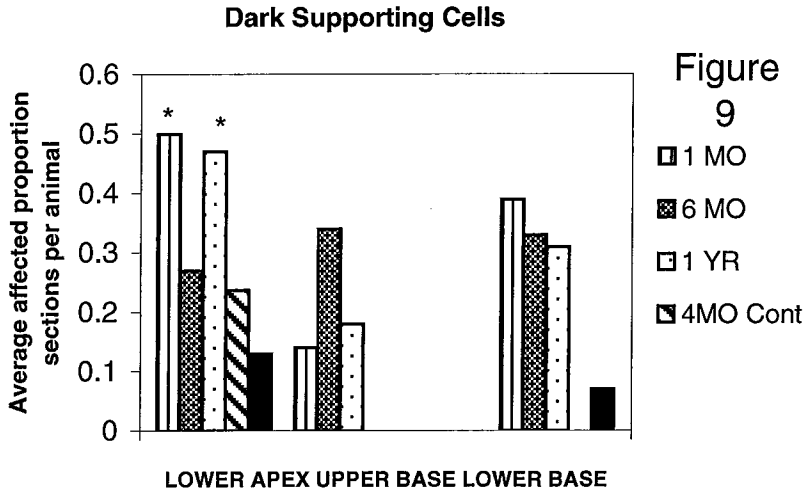
Dark Supporting Cells
Average affected proportion sections per animal
0.6
0.5
0.4
0.3
0.2
0.1
0
*
*
LOWER APEX
UPPER BASE
LOWER BASE
1 MO
6 MO
1 YR
4MO Cont

Figure 9